

Anisotropies and Chemical Composition of Ultra-High Energy Cosmic Rays Using Arrival Directions Measured by the Pierre Auger Observatory

EDIVALDO M. SANTOS¹, FOR THE PIERRE AUGER COLLABORATION²

¹*Instituto de Física, Universidade Federal do Rio de Janeiro, 21941-972, Rio de Janeiro, Brazil*

²*Observatorio Pierre Auger, Av. San Martin Norte 304, 5613 Malargüe, Argentina*

(Full Author list: http://www.auger.org/archive/authors_2011_05.html)

auger_spokespersons@fnal.gov

Abstract: The Pierre Auger Collaboration has reported evidence for anisotropies in the arrival directions of cosmic rays with energies larger than $E_{th} = 55$ EeV. There is a correlation above the isotropic expectation with nearby active galaxies and the largest excess is in a celestial region around the position of the radio galaxy Cen A. If these anisotropies are due to nuclei of charge Z , the protons accelerated in those sources are expected, under reasonable assumptions, to lead to excesses in the same regions of the sky at energies above E_{th}/Z . We here report the lack of anisotropies at these lower energies for illustrative values of $Z = 6, 13$ and 26 . These observations set stringent constraints on the allowed proton fraction at the sources.

Keywords: Ultra-High Energy Cosmic Rays, Anisotropies, Chemical Composition, Pierre Auger Observatory

1 Introduction

Measurements of the anisotropies in the distribution of arrival directions of Ultra-High Energy Cosmic Rays (UHECR), when combined with information on their chemical composition and spectral features can provide valuable information on the sources and acceleration mechanisms capable of producing subatomic particles with macroscopic energies.

The Pierre Auger Observatory, the largest cosmic ray detector ever built, has observed [1] a flux suppression above 40 EeV (where $1 \text{ EeV} = 10^{18} \text{ eV}$) consistent with that expected from the interaction of protons or heavy nuclei with the cosmic microwave background [2, 3]. In addition, it has reported evidence for anisotropy in the distribution of arrival directions of the highest energy events [4, 5, 6]. The arrival directions of the events with energies above 55 EeV show a degree of correlation within an angular scale of $\sim 3^\circ$ with the positions of nearby (within ~ 75 Mpc) AGN from the VCV catalog [7], which is above that expected from chance coincidences in an isotropic sky. However, one cannot identify AGN as the actual sources of UHECR since these trace the distribution of matter in the local Universe where other potential acceleration sites (such as Gamma Ray Bursts) are also present. Another interesting feature observed in the data sample is an excess of arrival directions towards the celestial position of Cen A, which is most significant in an angular window of radius 18° . This is the nearest radio loud AGN at \sim

4 Mpc from Earth, and is located at equatorial coordinates $(\alpha, \delta) = (201.4^\circ, -43.0^\circ)$.

The determination of the composition of primary CRs at the energies for which their flux is measured to be strongly suppressed is an active area of study. This stems from both the low observed flux and the reliance on Monte Carlo models that require large extrapolations from currently measured physics. A method was recently proposed linking the anisotropy and composition measurements by exploiting that particles with the same rigidity follow the same path through a magnetic field [8]. Given generic assumptions about the acceleration process at the source, neglecting interactions with the photon background and assuming that the anisotropies at energies E are caused by heavy primaries with charge Z , it relates the strength of an anisotropy at energy E/Z to the fraction of protons at that energy in the same source. We here describe observations related to a search for this kind of effect using data collected by the Pierre Auger Observatory [9].

2 The Detector and the Data Sample

Located in the city of Malargüe, Mendoza, Argentina, the Pierre Auger Observatory is a hybrid detector formed by a Surface Detector (SD) with 1660 stations covering an area of $\sim 3000 \text{ km}^2$ and a Fluorescence Detector (FD) comprised of 27 fluorescence telescopes in four locations around the border and overlooking the array. As the shower develops in the atmosphere, the nitrogen scintillation light

is detected by the telescopes which are able to record the ultraviolet radiation emitted during the de-excitation of molecular nitrogen. When shower particles reach ground level they are detected through water-Cherenkov light produced within the SD stations [10].

The reconstruction of the event direction is done by fitting a certain shower front model propagating at the speed of light to the measured arrival times and particle densities in the stations triggered by the air shower. By profiting from the unique hybrid nature of the Auger Observatory, events which are detected simultaneously by the SD and the FD are used to inter-calibrate these two detectors, providing an energy estimate almost independent of Monte Carlo simulations. Firstly, the estimated signal at 1000 m from the reconstructed shower core, $S(1000)$, is corrected for atmospheric attenuation, and gives rise to a signal value at a reference zenith angle (S_{38}). Finally, this signal can then be correlated to the calorimetric energy measurement performed by the FD. Such a calibration curve has been determined for the hybrid events and can be used for the whole high statistics sample measured by the SD [11].

The data used in this analysis were collected by the SD from 1 January 2004 to 31 December 2009 and contain showers with reconstructed zenith angle $\theta < 60$ degrees. Only events for which the station with the highest signal was surrounded by an entire hexagon of active detectors at the time of detection have been included. Recording the number of active detector configurations able to trigger such showers allows one to obtain the array exposure as a function of time. Also, by monitoring the communications between individual stations and the Central Data Acquisition System, we are able to identify dead times in the detectors. After accounting for these and removing periods of large fluctuations in the array aperture we are left with a livetime for the SD array of about 87%.

3 Low Energy Anisotropy Searches

In ref. [8], Lemoine and Waxman explored the consequences of the assumption that the anisotropies observed at the highest energies (above a threshold E_{th}) were caused by a predominantly heavy component. Assuming the presence of protons in the same source, and considering the fact that the Larmor radius in a given magnetic field depends only on rigidity, E/Z for relativistic particles, if the high energy anisotropy is due to particles with charge Z there should be a corresponding low energy anisotropy of protons at energies above E_{th}/Z .

In ref. [6] the most significant excess for a top-hat window centred on Cen A was found for a radius of 18° , and we will hence focus on this region. There are a total of 60 events in this data set, and 10 are at a distance smaller than 18° of the position of Cen A¹. The number of events expected by random correlations in a completely isotropic sky, taking into account also the detector exposure, is estimated as $N_{bkg} = (N_{tot} - N_{obs})x/(1 - x) = 2.44$, where

$x \simeq 0.0466$ is the fraction of the sky, weighted by the observatory's exposure, covered by the 18° circular window around Cen A. The *a posteriori* nature of the observed excess around Cen A (the location of the excess, the energy threshold and angular size were chosen so as to maximize the excess) implies that new independent data will be required to determine the actual strength of the source and establish its significance in an *a priori* way.

Taking as representative values for the atomic number of heavy primaries $Z = 6, 13$ and 26 , we have searched for anisotropies in an 18° window around Cen A above threshold energies of $E_{th}/Z = 9.2$ EeV, 4.2 EeV and 2.1 EeV, respectively. Table 1 presents the total, observed, and expected number of events adopting different values of Z . No significant excesses have been found.

Z	E_{min} [EeV]	N_{tot}	N_{obs}	N_{bkg}
6	9.2	4455	219	207 ± 14
13	4.2	16640	797	774 ± 28
26	2.1	63600	2887	2920 ± 54

Table 1: Total number of events, N_{tot} , and those observed in an angular window of 18° around Cen A, N_{obs} , as well as the expected background N_{bkg} . Results are given for different energy thresholds, corresponding to $E_{min} = E_{th}/Z$ for the indicated values of Z and $E_{th} = 55$ EeV.

Above an energy of $E_{th} = 55$ EeV, the arrival directions measured by Auger have a degree of correlation above isotropic expectations with the positions of nearby AGN in the VCV catalog at less than 75 Mpc ($z_{max} = 0.018$) in an angular window of 3.1° [6]. Therefore, we have also looked for anisotropies above the same low energy thresholds for events in $\psi = 3.1^\circ$ windows around the same VCV AGN. Once again, no statistically significant excesses have been identified and a summary of the searches is shown in table 2. It is worth mentioning that the data collected during the exploratory scan, i.e., the period during which the collected data were used to tune the correlation parameters (E_{th}, z_{max}, ψ) in order to maximize the correlation signal (see [6] for details), were not used to produce this table.

Z	E_{min} [EeV]	N_{tot}	N_{obs}	N_{bkg}
6	9.2	3626	763	770 ± 28
13	4.2	13482	2852	2860 ± 54
26	2.1	51641	10881	10966 ± 105

Table 2: Total number of events, N_{tot} , and those observed within 3.1° from objects with $z \leq 0.018$ in the VCV catalog, N_{obs} , as well as the expected isotropic background N_{bkg} . Results are given for different energy thresholds, corresponding to $E_{min} = E_{th}/Z$ for the indicated values of Z and $E_{th} = 55$ EeV.

1. In ref. [6], 13 out of 69 arrival directions are reported within 18 deg. of Cen A. The difference with the numbers reported here is due to a stricter event selection necessary for an accurate estimate of the exposure at low energies.

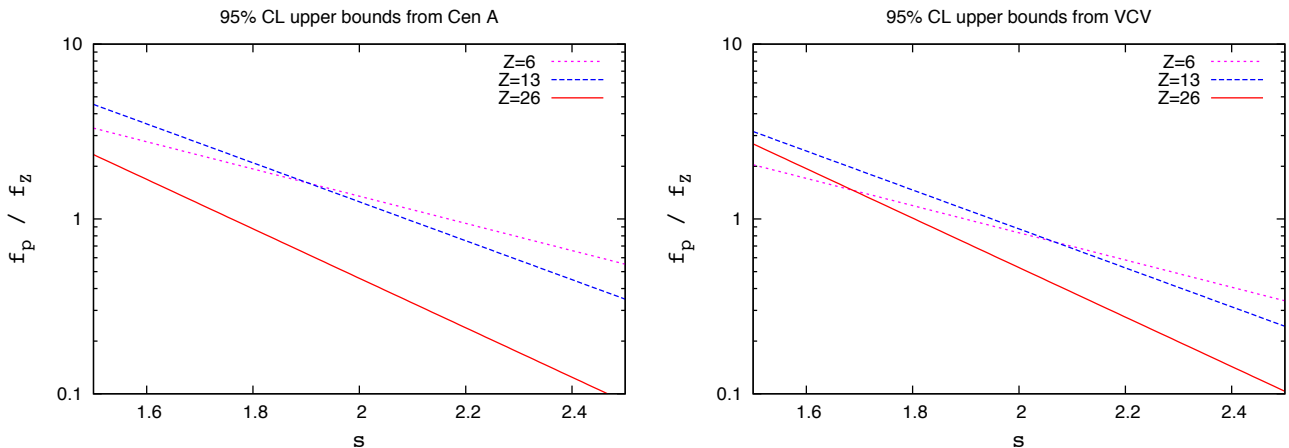


Figure 1: Upper bounds at 95%CL on the allowed proton to heavy fractions in the source as a function of the assumed low energy spectral index s . The different lines are for charges $Z = 6, 13$ and 26 , as indicated. Left: bounds from Cen A analysis. Right: bounds from VCV analysis.

For the heaviest primaries considered here ($Z = 26$), the low energy threshold (2.1 EeV) falls below the region of full SD efficiency ($E > 3$ EeV). In this case, we have performed a fit to the observed zenith angle distribution of the events in order to account for the zenith angle dependent detection efficiency in the estimate of the isotropic expectations in the windows considered.

4 Chemical Composition Constraints

In astrophysical environments for which the acceleration processes are essentially dependent on the magnetic rigidity, one can write the differential cosmic ray energy spectrum for primaries of atomic number Z as:

$$\frac{dn_Z}{dE} = k_Z \Phi \left(\frac{E}{Z} \right),$$

where k_Z is a normalization constant for the spectrum. Under this assumption, the expected number of protons $N_p(E > E_{th}/Z)$ above E_{th}/Z can be shown to be related to the number of heavy primaries $N_Z(E > E_{th})$ above E_{th} through $N_p(E > E_{th}/Z) = \frac{k_p}{Zk_Z} N_Z(E > E_{th})$. Experimentally one can estimate the ratio of source event numbers above the low and high energy thresholds as

$$R_Z \equiv \frac{N(E > E_{th}/Z)}{N(E > E_{th})},$$

where $N = N_{obs} - N_{bkg}$. The numerator of this ratio is equal to the sum of protons ($N_p(E > E_{th}/Z)$) and heavy nuclei ($N_Z(E > E_{th}/Z)$), whereas the denominator is considered to be dominated essentially by heavy primaries, i.e., $N_Z(E > E_{th})$. Therefore, a conservative upper bound on the ratio is $R_Z > \frac{k_p}{Zk_Z} + 1$, where no extra assumption was made on the spectral shapes of both chemical species. This inequality can be interpreted as a lower bound on the spectral normalizations $k_p/k_Z < (R_Z - 1)Z$.

We use the profile likelihood method [12] to derive upper bounds on the ratio R_Z both for events around Cen A and those around the positions of the VCV AGN. This method takes into account Poisson fluctuations in the signal and expected background at both high and low energies simultaneously. We find the following 95% CL bounds:

$$R_{26}^{\text{CenA}} < 12.9, \quad R_{13}^{\text{CenA}} < 17.3, \quad R_6^{\text{CenA}} < 9.1$$

$$R_{26}^{\text{VCV}} < 14.7, \quad R_{13}^{\text{VCV}} < 12.4, \quad R_6^{\text{VCV}} < 6.0$$

If we now assume that below a certain cutoff E_1 the energy spectra are proportional to power laws of rigidity, one can write

$$\Phi \left(\frac{E}{Z} \right) \propto \left(\frac{E}{Z} \right)^{-s}$$

and the ratio of spectral normalizations can be written in terms of the relative abundances of protons to species of charge Z at the sources $\frac{f_p}{f_Z} = \frac{k_p}{k_Z} Z^{-s}$.

Figure 1 shows the corresponding upper limits on the proton to heavy primary abundances at the sources as a function of the spectral index s for different Z . The bounds obtained from the analysis of Cen A are similar to those obtained from VCV AGN, becoming more stringent as the spectral index hardens. Even though we have not included energy losses in this analysis, these will eventually degrade the energy of the high energy nuclei, increasing the size of the predicted low energy anisotropy [8]. Therefore, the bounds discussed here are conservative.

Since the size of the angular window around Cen A was chosen *a posteriori*, an unbiased estimate of the significance will only be found with new independent data. However, it is worth mentioning that varying the energy threshold to 50 or 60 EeV leads to similar results. Also, varying the angular window to 10° has no large impact on the bounds, with the main effects coming from the change in the expected background, the limits being relaxed by a factor ~ 2 in this case.

5 Conclusions

We have presented observations of the distribution of events at energies above E_{th}/Z in the directions where anisotropies have been previously observed above $E_{th} = 55$ EeV. We pursued the idea that the anisotropies at high energies could be caused by heavy primaries, either for the excess of events around Cen A at an angular scale of 18° or for an angular scale of 3.1° around the positions of VCV AGN. We have taken as representative values for the atomic numbers present in sources $Z = 6, 13,$ and 26 . The low energy (E_{th}/Z) anisotropy caused by the protons in the same source are not observed, allowing us to impose upper bounds on the light to heavy composition abundances at the source. The bounds from both the VCV and the Cen A analyses are similar, and their dependence with the source spectral index is such that softer spectra produce less stringent upper limits. Low energy abundance measurements have been performed by the ATIC-2 experiment [13] and they point to f_p/f_Z values, as measured on Earth, above the upper limits presented here (for example, $f_p \simeq f_{He} \simeq 2f_{CNO} \simeq 2f_{Ne-Si} \simeq 2f_{Z>17} \simeq 4f_{Fe}$). At these low energies (100 TeV), cosmic rays are believed to be of galactic origin, and the larger diffusion coefficient of protons in our galaxy's magnetic field as compared to heavier nuclei imply that the corresponding f_p/f_Z at the sources are even larger. However, the probable extragalactic origin of UHECR, as well as their much higher energies, implies that the ATIC measured abundances do not necessarily apply to the sources contributing to the Auger data and should be taken only as indicative values of the expected ratios.

Therefore, scenarios in which a rigidity dependent acceleration mechanism leads to a heavy primary domination at the highest energies and in which there is an abundant proton component at low energies (see Fig. 1) are not favored. How these conclusions are modified in the presence of strong structured magnetic fields and taking into account the relevant energy losses remains to be seen. Finally, we mention that this joint composition-anisotropy study is independent of measurements of the average depth of the maximum of shower development [14, 15]. Instead, it depends on assumptions related to propagation and acceleration mechanisms at the sources.

References

- [1] The Pierre Auger Collaboration, Phys. Lett. B, 2010, **685**: 239.
- [2] K. Greisen, Phys. Rev. Lett., 1966, **16**: 748.
- [3] G. T. Zatsepin, V. A. Kuz'min, Sov. Phys. JETP Lett., 1966, **4**: 78.
- [4] The Pierre Auger Collaboration, Science, 2007, **318**: 938.
- [5] The Pierre Auger Collaboration, Astropart. Phys., 2008, **29**: 188; Erratum-ibid., 2008, **30**: 45.
- [6] The Pierre Auger Collaboration, Astropart. Phys. 2010, **34**: 314.
- [7] M.-P. Véron-Cetty, P. Véron, Astron. & Astrophys. 2006, **455**: 773.
- [8] M. Lemoine and E. Waxman, JCAP, 2009, **11**: 009.
- [9] The Pierre Auger Collaboration, JCAP in press, 2011.
- [10] The Pierre Auger Collaboration, Nucl. Instr. and Meth. in Physics Research, 2010, **A613**: 29.
- [11] The Pierre Auger Collaboration, Phys. Rev. Lett., 2008, **101**: 061101.
- [12] W. A. Rolke, A. M. López, J. Conrad, Nucl. Instrum. and Meth. in Physics Research, 2005, **A551**: 493.
- [13] A. Pavnov et al., (ATIC-2 Collaboration), Bull. Russ. Acad. Sc.: Physics, 2007, **71**: 494; ibidem Physics, 2009, **73**: 564.
- [14] The Pierre Auger Collaboration, Phys. Rev. Lett., 2010, **104**: 091101.
- [15] The High Resolution Fly's Eye Collaboration, Phys. Rev. Lett., 2010, **104**: 161101.